Pharmaceutical Research, Vol. 26, No. 4, April 2009 (© 2008)
DOI: 10.1007/s11095-008-9795-9

Research Paper

A Novel Camptothecin Derivative Incorporated in Nano-Carrier Induced Distinguished Improvement in Solubility, Stability and Anti-tumor Activity Both *In Vitro* and *In Vivo*

Min Han,[1] Cai-Xia He,[1] Qiu-Li Fang,[1] Xiao-Chun Yang,[2] Yuan-Yuan Diao,[1] Dong-Hang Xu,[3] Qiao-Jun He,[2] Yong-Zhou Hu,[4] Wen-Quan Liang,[1] Bo Yang,[2] and Jian-Qing Gao[1,5]

Received August 8, 2008; accepted November 12, 2008; published online December 2, 2008

Purpose. An oil/water nanoemulsion was developed in the present study to enhance the solubility, stability and anti-tumor activity of a novel 10-methoxy-9-nitrocamptothecin (MONCPT).
Materials and Methods. MONCPT nanoemulsion was prepared using Lipoid E80 and cremophor EL as main emulsifiers by microfluidization. The droplet size of the nanoemulsion was measured by dynamic light scattering. *In vitro* drug release was monitored by membrane dialysis. Kinetics of MONCPT transformed into carboxylic salt was performed in phosphate buffer at different pH. Hemolysis of MONCPT nanoemulsion was conducted in rabbit erythrocytes. Solubilization character of MONCPT in nanoemulsion was experimented using Nile red as a solvatochromic probe. *In vitro* cytotoxicity of the nanoemulsion was measured in A549 and S180 cells using Sulforhodamine B protein stain method, and suppression rate of tumor growth was investigated in S180-bearing mice. The cell cycle effects of MONCPT nanoemulsion on S180 cells were analyzed by flow cytometry. Distribution of the nanoemulsion in A549 cells and S180-bearing mice were also investigated by fluorescence image.
Results. MONCPT is incorporated in the nanoemulsion in form of lactone with concentration of 489 μg/ml, more than 200 folds higher than that in water. Experiments using Nile red as a solvatochromic probe indicated that more MONCPT might be located in the interfacial surfactant layer of the nanoemulsion than that in discrete oil droplet or continuous aqueous phase. Nanoemulsion could release MONCPT in a sustained way, and it was further shown to notably postpone the hydrolysis of MONCPT with longer hydrolysis half-life time (11.38 h) in nanoemulsion at pH 7.4 than that of MONCPT solution (4.03 h). No obvious hemolysis was caused by MOCPT nanoemulsion in rabbit erythrocytes. MONCPT nanoemulsion showed a marked increase in cytotoxic activity, 23.6 folds and 28.6 folds in S180 cells and A549 cells respectively *via* arresting the cell at G2 phase, compared to that induced by MONCPT injection. It correlated well to the *in vivo* anti-tumor activity of MONCPT nanoemulsion with suppression rate of 93.6%, while that of MONCPT injection was only 24.2% at the same dosage. Moreover, nanoemulsion exhibited enhanced capability of delivering drug into malignant cell's nucleus *in vitro* and induced drug accumulation in tumor in S180-bearing mice using *in vivo* imaging.
Conclusion. The nanoemulsion prepared exhibited an improved MONCPT solubility, stability and anti-tumor activity, providing a promising carrier for cancer chemotherapy using MONCPT.

KEY WORDS: 10-Methoxy-9-nitrocamptothecin (MONCPT); anti-tumor; fluorescence; nanoemulsion; nile red.

INTRODUCTION

Known as important anticancer drugs, camptothecin derivatives, such as irinotecan, GG-211, dx-8951f, topotecan, 9-nitrocamptothecin and 10-hydroxycamptothecin have attracted extensive attention for their binding and inhibition of topoisomerase I (Topo I) which distributed extensively in tumor cells (1,2). However, the response rate and overall survival rate have not been improved substantially for most of them compared to that of camptothecin (3). Although 9-nitrocamptothecin possesses a potent activity with low toxicity, difficult in preparing limits its research and clinical application. The introduction of a nitro at position 9, such as 9-nitrocamptothecin, has shown satisfactory activity with low toxicity. However, 9-nitrocamptothecin was difficult to prepare by nitration of camptothecin because 12-nitrocamptothecin was the main product (4). In contrast, 10-alkoxy-9-nitrocamptothecin (MONCPT) could easily be prepared from 10-

[1] Institute of Pharmaceutics, College of Pharmaceutical Sciences, Zhejiang University, Hangzhou, China.
[2] Institute of Pharmacology & Toxicology and Biochemical Pharmacy, College of Pharmaceutical Sciences, Zhejiang University, Hangzhou, China.
[3] 2nd Affiliated Hospital of Zhejiang University School of Medicine, Hangzhou, China.
[4] Institute of Material Medica, College of Pharmaceutical Sciences, Zhejiang University, Hangzhou, China.
[5] To whom correspondence should be addressed. (e-mail: gaojianqing@zju.edu.cn)

hydroxycamptothecin (5,6), which possesses a potent anti-tumor activity due to its regulation of cell cycle or potential property for inhibiting angiogenesis as revealed in our previous studies (7,8). However, poor solubility and stability of MONCPT like other camptothecin derivatives limits its further *in vivo* researches. Although transformation of a lactone ring contained in camptothecin derivatives into an open-ring hydroxy carboxylic acid in alkaline solvents may enhance its solubility dramatically, an inevitable decrease in activity or increase in toxicity makes it inappropriate for application (9–11).

Meanwhile, considerable emphasis has been given to develop emulsion systems as drug carrier system because of its improved solubilization for water-insoluble and/or oil insoluble active compounds, modified drug release characteristic, protecting drug from transformation and delivering drugs into some tissues specifically after intravenous administration (12–16). Being a class of stable emulsions composed of discrete oil phase and continuous aqueous phase separated by a monolayer of surfactants with particle diameter usually less than 100 nm (17), nanoemulsion have been shown to increase bioavailability and efficacy of a number of compounds such as insulin and paclitaxel (18,19).

In present study, nanoemulsion incorporating MONCPT was developed to achieve a potential parenteral delivery system for MONCPT. The investigation focuses on the release and stability of the drug encapsulated in nanoemulsion, as well as its anti-tumor activity both *in vitro* and *in vivo*. Furthermore, Nile red was used as a solvatochromic probe to investigate the mechanism of solubility enhancement, and the distribution of nanoemulsion in cell nucleus and in tumor-bearing animals.

MATERIALS AND METHODS

Materials

Lipoid E80 was purchased from Lipoid AG (Ludwigshafen, Germany), which consists of 82.4% phosphatidylcholine and 8.0% phosphatidyl ethandamine as mentioned in manufacture's specification. Cremophor EL was furnished by BASF (Parsippany, NJ.USA). Soybean oil was purchased from Tielingbeiya pharmaceutical Co. (Tieling, China). Glycerol formal was kindly provided by Elementis (London, England). Sulforhodamine B (SRB) was purchased from Sigma (St Louis, MO, USA). All other chemicals and reagents used were of analytical or chromatographic grade.

Assay of MONCPT

High performance liquid chromatography (HPLC) system was composed of an Agilent G1310A pump, an Agilent G1314A VWD detector and a Diamonsil® C18 reverse phase column(4.6× 150 mm, 5 um, Dikma Technologies). The mobile phase consisted of acetonitrile-1% triethylamine in distilled water (32:68) with pH adjusted to 5.5 by glacial acetic acid. Chromatography was performed at 40°C and wavelength was set to 383 nm.

Preparation of MONCPT Nanoemulsion

Mass samples of 0.27 g lipoid E80, 0.36 g cremophor EL, 0.15 g ethanol, and 15 mg MONCPT were dissolved into 1.8 g soybean oil at 70°C. 6.0 g PEG 400, 0.66 g glycerol and 6.0 g glycerol formal were dissolved in 15 g purified water as aqueous phase. After mixing aqueous phase with oil phase at 70°C, The coarse nanoemulsion was obtained by homogenization using a FJ-200 high shear mixer (12,000 rpm, 3 min; Shanghai Specimen Model Ltd., Shanghai, China), then it was further emulsified in a M110L microfluidizer system (Microfluidics Co., American) under ten microfluidization cycles at a pressure of 12,000 psi at 4°C to obtain final nanoemulsion with MONCPT concentration of 0.489 mg/ml. Ethanol was used as co-surfactant, and PEG 400, glycerol formal were applied as solubilizer and stabilizer in the formulation.

Characteristic Evaluation of MONCPT and Nanoemulsion

Solubility of MONCPT in different solvents was measured by shaking 3 ml solvents added with excess amount of MONCPT at 37°C for 48 h away from light. The suspension was centrifuged at 8,000×*g* for 10 min and filtered through a 0.22 μm membrane, then MONCPT concentration in samples was determined by HPLC. N-octanol/water partition coefficient (*P*) of MONCPT was determined by shaking-flask method based on thorough mixing of the two phases to reach the equilibrium (20). Briefly, 5 ml MONCPT solution in n-octanol-saturated water (2.5 μg/ml) and 5 ml water-saturated *n*-octanol were pipetted into a 10 ml centrifuging tube, which then was incubated at 25°C with shaking at 50 rpm in an incubation shaker (THC-Z; Taicang laboratorial equipment factory, Jiangsu, China) for 24 hours away from light, followed by centrifuging (10,000 rpm, for 10 min) and the analysis of MONCPT in the aqueous phase with HPLC. Then N-octanol/water partition coefficient (*P*) values were calculated according to the equation followed. Where C_O and C_W are the concentration of MONCPT, and V_O, V_W are the volumes of n-octanol and distilled water, respectively.

$$P = \frac{C_O \cdot V_W}{C_w \cdot V_O} \quad (1)$$

Following appropriate dilution with distilled water, MONCPT nanoemulsion droplet size was determined by dynamic light scattering (MALVERN Nano ZS®, Malvern, UK). The nanoemulsion profiles was checked under JEM1230 electronmicroscope (Japan Electron Optics Laboratory, Tokyo, Japan) and pH was measured using a pH-meter at room temperature.

In vitro release of MONCPT was monitored by reversed-dialysis bag method at 37°C under shaking at 75 rpm using phosphate-buffered saline (PBS; 10 mM) as a sink solution at pH 7.0 (21). Dialysis bag with a MW cut-off between 12k and 14k was filled with 10 ml PBS and immersed into 250 ml PBS to equilibrium for 12 h, then 1 ml MONCPT nanoemulsion, 1 ml MONCPT injection (Distilled water dissolved MONCPT at 0.5 mg/ml with pH adjusted to 8.0 by NaOH after addition of 0.1‰ EDTA and 1‰ $NaHSO_3$, and then filtered through 0.22 μm membrane), and 1 ml MONCPT water solution (0.5 mg/ml, containing 5% DMSO) were added into 250 ml blank PBS outside of dialysis bag, respectively. At predetermined intervals, 200 μL samples were taken from release medium inside of dialysis bag followed by immediate replacement with 200 μL fresh PBS. Drug release profiles (% drug released *vs* time) were generated. Assuming 100%

drug release, the concentration of MONCPT in the PBS will be <2 μg/ml which is lower than MONCPT water solubility 2.61 μg/ml.

Transformation kinetics of MONCPT in PBS at different pH was investigated. 20 μl MONCPT water solution (containing 25% DMSO; 1 mg/ml) or 15 μl MONCPT nanoemulsion (0.489 mg/ml) was added up to 10 ml with PBS at various pH (5.5, 6.4, 7.4, 8.0). 50 μl samples was taken at predetermined intervals and rapidly measured by HPLC.

Hemolysis Study

After blood clotting by rotation under assist of glass beads, blood samples, obtained from rabbit arteria auricularis, were immediately separated by centrifugation at 2,000 rpm for 10 min and washed three times with saline. Then, erythrocytes were collected and diluted with saline to 2% suspension. 0.3 ml MONCPT nanoemulsion or injection was added to tubes and the volume was adjusted to 2.5 ml with saline, and then incubated with 2.5 ml 2% erythrocyte suspension at 37°C. After 3 h of incubation, the samples were centrifuged for 10 min at 2,000 rpm. The percentage of hemolysis was determined by comparing the absorbance at 414 nm of the supernatant with that of positive control samples totally hemolyzed with distilled water (taken as 100%), and hemolysis induced with saline was used as negative control.

Solubility Characteristic of Nanoemulsion

Nile red (Sigma, St Louis, MO, USA) was used as a solvatochromic and hydrophobic probe to investigate the solubility characteristic of the nanoemulsion. An excess amount of Nile red powder was added into (1) soybean oil that was used as oil phase in the nanoemulsion, (2) solution with the same components of aqueous phase in the nanoemulsion, and (3) nanoemulsion that was prepared as described in the text with MONCPT removed, respectively. These solutions were sonicated for 20 min and were left for 24 h away from light, then the supernatants were obtained by centrifugalization at 12,000 rpm for 10 min. After standard curve of Nile red dissolved in 1-propanol (Beijing chemical plant, China) was established by UV-VIS absorbance at 546 nm in a TU-1800PC Scanning Spectrophotometer (Puxi GP Co. BeiJing, China), Nile red concentration in the supernatants diluted by 1-propanol appropriately was determined. On the other hand, absorbance spectra of Nile red in the above solutions was also performed to explore the location site of Nile red in the nanoemulsion according to the approach described previously (22).

In Vitro and *In Vivo* Anti-Tumor Activity

A549 and S180 cell lines were obtained from ATCC and grown in Dulbecco's modified Eagle's medium with 10% fetal calf serum in 96-well cell-culture plates under 5% CO_2 at 37°C for 48 h. The *in vitro* cytotoxicity of the nanoemulsion, injection and water solution (containing 1‰ DMSO) of MONCPT in A549 and S180 cells was measured using Sulforhodamine B (SRB) protein stain method (23). MONCPT-free nanoemulsion (same composition of the nanoemulsion without MONCPT) was also detected to evaluate the potential side effects of the components in the nanoemulsion.

Male mice (10 mice per group) were subcutaneously implanted with 0.2 ml S180 ascites tumor cells (1×10^6 cells/ml). Twenty four hours after implantation, mice were randomly sorted into treatment groups and were administrated intravenously (i.v.) with saline (10 ml/kg), MONCPT nanoemulsion (5 mg/kg), MONCPT injection (5 mg/kg), intramuscularly (i.m.) with MONCPT oil (tea oil, 10 mg/kg) suspension, and intraperitoneally (i.p.) with cyclophosphamide (30 mg/kg) once every 2 days. Tumors were removed from sacrificed mice at day 16 post inoculation, and were weighed to evaluate antitumor activity of various treatments. The percentage of tumor growth was calculated as equation followed:

$$\text{Suppression rate } (\text{SR}\times 100\%) = \frac{(W_c - W_t)\times 100}{W_c} \qquad (2)$$

Where W_c and W_t are the mean tumor weights (grams) of the control and the treated mice respectively.

DNA Cell Cycle Analysis by Flow Cytometry

To analysis cell cycle, S180 cells (5×10^4 cells/ml, 5 ml) were cultured in 25 cm^2 flasks, treated with the nanoemulsion incorporating MONCPT (0.2, 0.4, 0.8 mM) for 24 h. Cells were then harvested and quickly washed twice with ice-cold PBS, and cell pellets were resuspended in 1 ml of 0.1% sodium citrate containing propidium iodide (PI) 0.05 mg and 50.0 μg RNase for 30 min at room temperature in the dark. Flow cytometry was performed on a Becton Dickinson FACScan, with collection and analysis of data performed using Becton Dickinson CELLQuest software.

Fluorescence Microscopy

Nile red was used as a substitute for MONCPT to prepare nanoemulsion at a final concentration of 0.1 mg/ml, which was employed to investigate the influence of nanoemulsion on Nile red uptake in tumor cells and distribution in depilated mice bearing S180 cells.

After being incubated with Nile red nanoemulsion that had been diluted to 250 times volume by PBS for 0.5 h, A549 cells were washed with PBS for three times to remove Nile red that had not been absorbed. In order to demonstrate the intracellular location of Nile red, which could emit red fluorescence at an excitation wavelength of 543 nm, the same A549 cells were further incubated with Hoechst 33342 (Beyotime institute of biotechnology, Jiangsu, China) in Hank's Balanced Salt Solution (HBSS; 2 μg/ml) for 10 min to specifically stain the cell nucleus blue with an excitation wavelength of 346 nm. Same conduction was performed for Nile red in HBSS (containing 1% DMSO) as control to Nile red nanoemulsion. After incubation, the A549 cells were monitored by fluorescence microscopy, and images of red fluorescence of Nile red and blue fluorescence of hoechst 33342 were overlapped to investigate the intracellular distribution of Nile red.

For *in vivo* imaging, male mice were subcutaneously implanted with 0.2 ml S180 ascites tumor cells (1×10^6 cells/ml). Ten days after implantation, mice were depilated and i.v. Nile red nanoemulsion. Then the *in vivo* image of Nile red

fluorescence was observed in MATSTRO Live Animal Multispectral Imaging System (CRI Co.).

Statistical Analysis

Values are expressed as mean±SD. Statistical comparisons were made by using two-tailed Student's *t*-test and comparisons among more than three groups were performed by using one-way ANOVA. $P<0.05$ was considered to be significant.

RESULTS

Characteristics of MONCPT and Nanoemulsion

As determined by HPLC, solubility of MONCPT in water, methanol, n-octanol, Migylol 812, glyceryl trioleate and soybean oil is 2.61, 69.47, 19.46, 13.71, 17.18 and 17.47 μg/ml respectively, and *N*-octanol/water partition coefficient (*P*) is 3.82±1.31, which indicates the insolubility of MONCPT in both hydrophilic and hydrophobic solvents. Content of MONCPT incorporated in the nanoemulsion was determined to be 489 μg/ml, which is significantly higher than that in water and oils as mentioned above. pH of the MONCPT nanoemulsion was tested to be 5.78, protecting MONCPT from transformation in alkaline circumstance. The image of MONCPT nanoemulsion observed under transmission electron microscope was shown in Fig. 1A. The particle size measured by dynamic light scattering ranged from 45 to 95 nm with a mean diameter of 67 nm.

Release kinetics of MONCPT from the nanoemulsion or injection was investigated using MONCPT water solution as control. There was no significant difference in release profiles between injection and water solution that release MONCPT rapidly as shown in Fig. 1B. While the nanoemulsion showed a relatively sustained way with less than 70% MONCPT being released over 4 h.

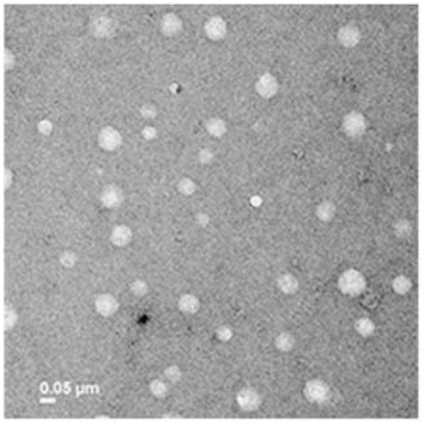

A

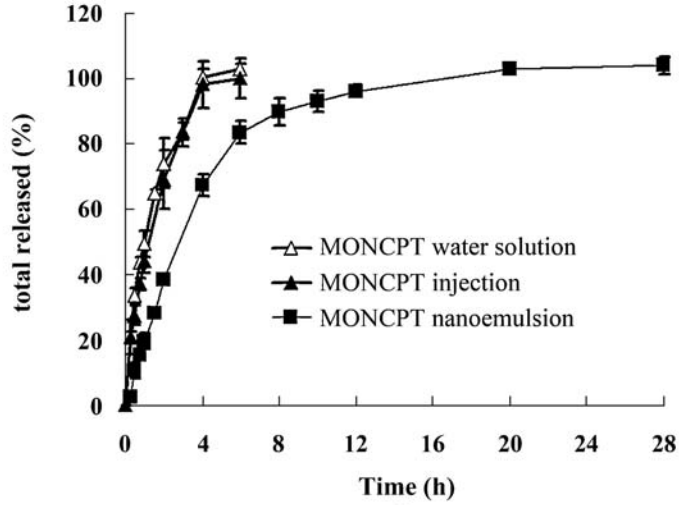

B

pH	$T_{1/2,h\ (Water)}$	$T_{1/2,h\ (Emulsion)}$
5.8	11.59	12.93
6.8	8.52	10.44
7.4	4.03	11.38
8.0	1.05	6.70

C

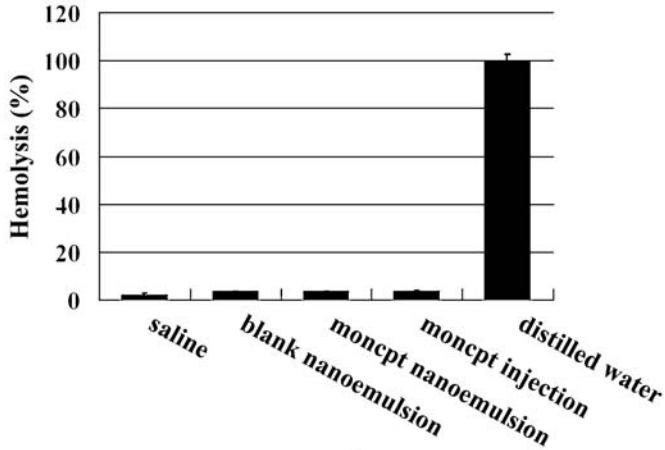

D

Fig. 1. Characteristics of MONCPT nanoemulsion. **A** Transmission electron microscope photograph of MONCPT nanoemulsion. **B** *In vitro* release of MONCPT from the nanoemulsion, injection and the water solution at 37°C under shaking (75 rpm) which was monitored by reversed-dialysis bag using phosphate-buffered saline (PBS) as a sink solution at pH 7.0. Each value represents the mean and SD($n=3$). **C** Half life ($T_{1/2}$) of MONCPT transformed into open-ring form after MOCPT water solution or MONCPT nanoemulsion was incubated in PBS at various pH. **D** Hemolysis percentage (%) in rabbit blood erythrocytes after incubation with blank nanoemulsion, MONCPT nanoemulsion and MONCPT injection for 3 h at 37°C with saline as negative control and distilled water as positive control (%; $n=3$).

It is known that lactone form is the main active form of camptothecin or its derivatives. Therefore, *in vitro* transformation of MONCPT into carboxylate form in PBS at various pH (5.8, 6.8, 7.4, 8.0) was measured to evaluate the potential contribution of nanoemulsion to stability enhancement of MONCPT in alkaline circumstance. The transformation of MONCPT basically followed first-order kinetics and half-life of hydrolysis ($T_{1/2}$) was showed in Fig. 1C as calculated form the linearity portion. Nanoemulsion could postpone the hydrolysis of MONCPT, and this protection is more prominent when MONPCT is exposed to alkaline medium with $T_{1/2,h}$ of 11.38 and 6.70 respectively in nanoemulsion at pH 7.4 and 8.0 comparing to that of 4.03 and 1.05 in water solution. The protection is benefit for curative effect of MONCPT because pH of blood in body is about 7.4 that may transform lactone form of MONCPT into a carboxylate form.

Safety significantly accounts in the evaluation of the quality and the potential clinical application of a drug delivery system. Therefore, hemolysis study was performed to investigate the potential *in vivo* irritation of nanoemulsion and injection of MONCPT. As shown in Fig. 1(D), there were no hemolysis or blood cell agglutination induced by nanoemulsion (containing MOCPT or not) and MONCPT injection within 3 h *in vitro*.

Solubility Characteristic of Nanoemulsion

For investigating the mechanism of solubilization effect of nanoemulsion, Nile red was used as the probe.The solubility of Nile red in aqueous phase and oil phase of nanoemulsion was 624.1 and 15.8 μg/ml respectively, while the solubility of Nile red in the nanoemulsion was tested to be 145.95 μg/ml, which is about twice more than total amount of Nile red dissolved in the discrete oil phase and continuous aqueous phase of the nanoemulsion. The wavelength at which maximum absorbance in the spectrum occurs is called λ_{max}, and λ_{max} of Nile red in the aqueous phase and oil phase was 585 and 523 nm, respectively. Meanwhile, nanoemulsion containing Nile red at 10 μg/ml exhibited λ_{max} of 526 nm, which is near to that in oil, indicating that Nile red locates mostly in the oil droplet of the nanoemulsion. In contrast, when Nile red in the nanoemulsion increased up to 100 μg/ml, λ_{max} shifts to 547 nm which suggests more of Nile red may be located in the interfacial surfactant layer between aqueous phase and oil phase (Fig. 2).

In Vitro and *In Vivo* Anti-Tumor Activity

MONCPT injection showed a significantly decreased growth inhibition on both A549 and S180 cells comparing to that induced by MONCPT dissolved in a lactone form in the water solution or nanoemulsion as shown in Fig. 3. And a bit more increased cytotoxicity of MONCPT nanoemulsion than MONCPT water solution was observed. Meanwhile, no cytotoxicity in A549 cell for MONCPT-free nanoemulsion was detected, whereas it was significant on S180 cells when MONCPT-free nanoemulsion of higher concentration was

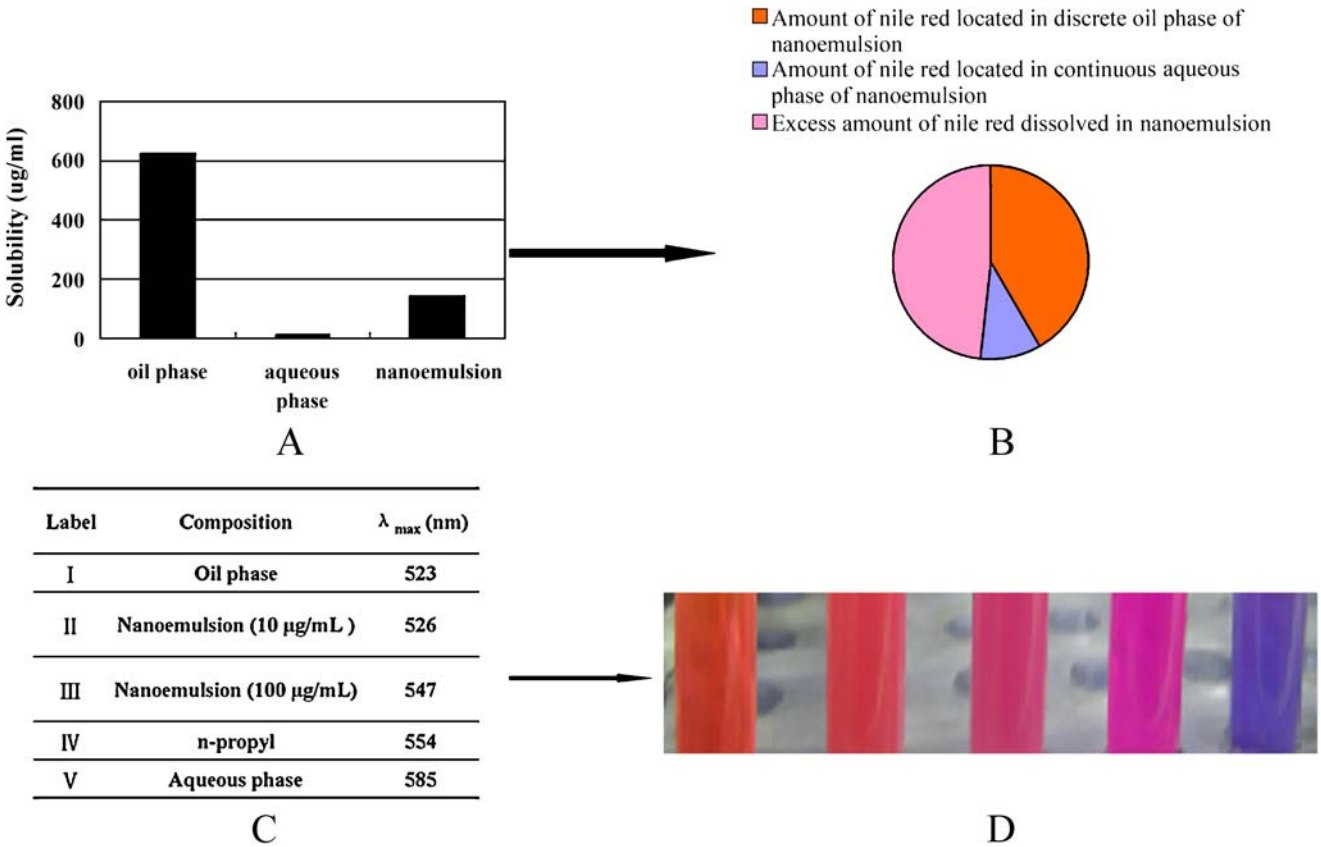

Label	Composition	λ_{max} (nm)
I	Oil phase	523
II	Nanoemulsion (10 μg/mL)	526
III	Nanoemulsion (100 μg/mL)	547
IV	n-propyl	554
V	Aqueous phase	585

Fig. 2. Solubility and UV-VIS absorbance of Nile red in various compositions of solvents. **A** the solubility of Nile red in oil phase, aqueous phase and nanoemulsion. **B** The solubilization effects on Nile red offered by nanoemulsion was demonstrated in the cake-like graph. **C** the wavelength of maximum absorbance (λ_{max}) of Nile red in various solvents. **D** Appearance of Nile red in five various solvents labeled with *I* to *V* as described in the (**C**).

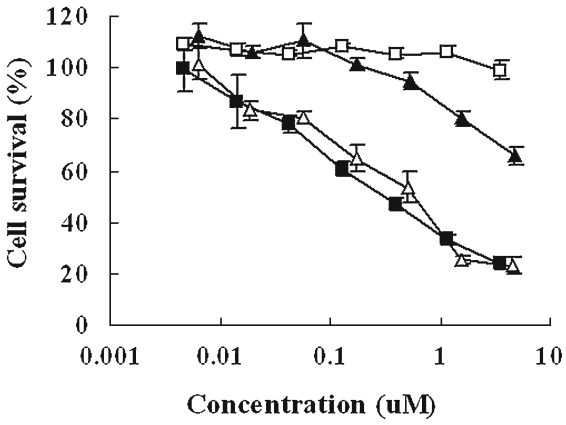

A

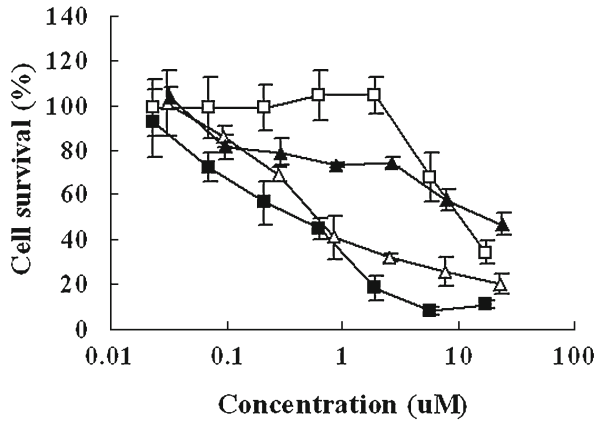

B

Cell lines	IC50 (μM)		
	Nanoemulsion	Water solution	Injection
A549	0.4126	0.5597	11.7880
S180	0.3414	0.4961	8.0572

C

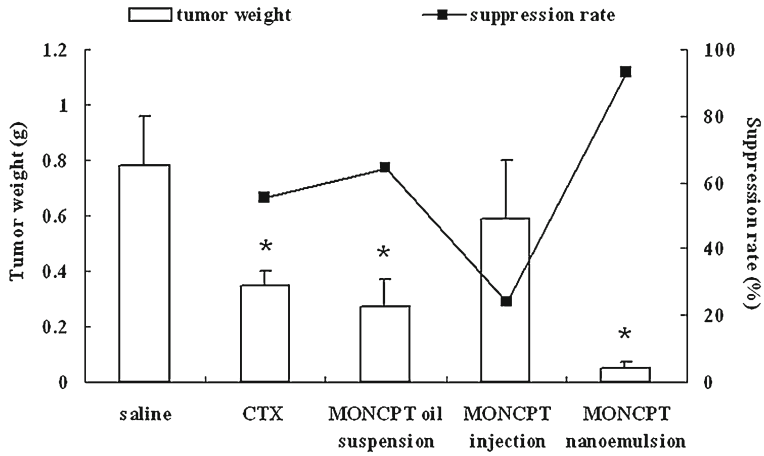

D

Fig. 3. *In vitro* and *in vivo* anti-tumor effect of MONCPT nanoemulsion. Survival rate of A549 (**A**) and S180 (**B**) cells exposing to MONCPT nanoemulsion (*filled square*), MONCPT-free nanoemulsion (same composition of the nanoemulsion without MONCPT) (*empty square*), MONCPT injection (*filled triangle*) and MONCPT water solution (*empty square*) for 24 h. Each value represents the mean and SD (n=4). Calculated 50% inhibiting concentration (IC50) was shown in the (**C**). **D** Suppression rate (%) of tumor weight after intravenous administration of saline (10 ml/kg; negative control), MONCPT nanoemulsion (5 mg/kg), MONCPT injection (5 mg/kg) and intramuscular administration of MONCPT oil suspension (10 mg/kg), and intraperitoneally administration of cyclophosphamide (CTX) solution (30 mg/kg) (positive control) for 2 weeks using S180-bearing mice (n=10). *P<0.05, compared with the negative control (saline).

used and this may be attributed to the variation of the cell sensitivity.

DNA damage caused by different agents induces cell cycle arrest at G1, S, or G2 thereby preventing replication of damaged DNA or aberrant mitosis. The cell cycle effects of MONCPT nanoemulsion were also studied in S180 cells as a function of drug concentration. 24 h after MONCPT nanoemulsion removal, S180 cells were arrested in G2 phase as shown in Fig. 4.

Since the low solubility of MONCPT in water can't enable the essential dose for i.v. administration in the *in vivo* anti-tumor studies, MONCPT dispersed in the tea oil as a

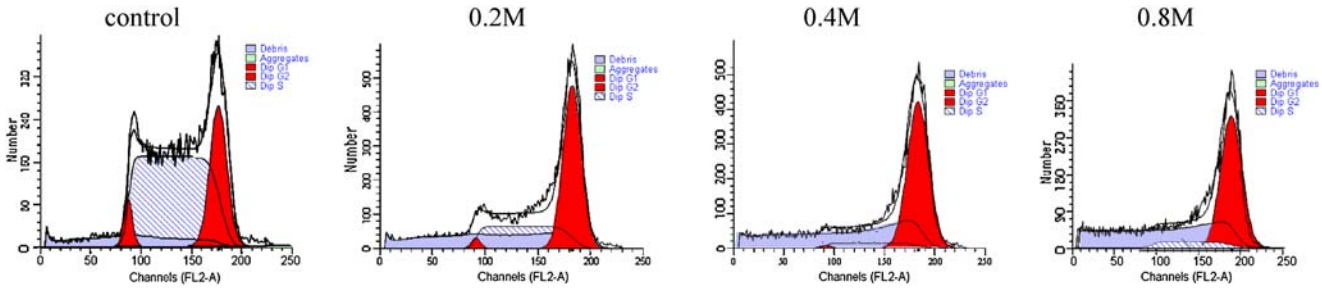

Fig. 4. Effects of MONCPT nanoemulsion on the cell cycle of S180 cells. Cells were treated with different concentration of MONCPT nanoemulsion (0.2, 0.4, 0.8 M) for 24 h and analyzed by flow cytometry after MONCPT nanoemulsion removal. Untreated S180 cells was used as control.

suspension was i.m. administrated as a control of lactone form of MONCPT to that of nanoemulsion. As shown in Fig. 3, MONCPT injection did not show notable tumor suppress effect (SR). In contrast, MONCPT oil suspension slightly increased the SR to 64.4% after i.m. administration at a dose of 10 mg/kg compared to that of Cyclophosphamide (55.6%) used as positive control. It is of interest to mention that a significantly enhanced anti-tumor activity (93.2%) was observed for MONCPT nanoemulsion after i.v. administration with only half dose of MONCPT oil suspension.

Fluorescence Studies

Efficient cellular uptake is necessary for anti-tumor agents to kill tumor cells. Therefore, intracellular distribution of drug was evaluated. As MONCPT emits no fluorescence, Nile red was applied and substituted for MONCPT in the nanoemulsion for its similarity of parent structure as MONCPT to some extent. Being a hydrophobic probe, Nile red could specifically dye intracellular lipids with red fluorescence. Hoechst 33342 was used to specifically dye the cell nucleus with blue for positioning. Seldom does Nile red pass across the hydrophilic nuclear membrane and distribute into the cell nucleus. This is testified in Fig. 5 by that there was no overlap of fluorescence for Nile red and hoechst 33342 in HBSS. As shown in Fig. 5, Nile red in nanoemulsion could distribute into A549 cell nucleus, suggesting the capability of delivering hydrophobic molecule into cell nucleus of the nanoemulsion. Furthermore, *in vivo* fluorescence image of Nile red in mice bearing S180 cells was also investigated. The results demonstrated that potent red fluorescence emitted

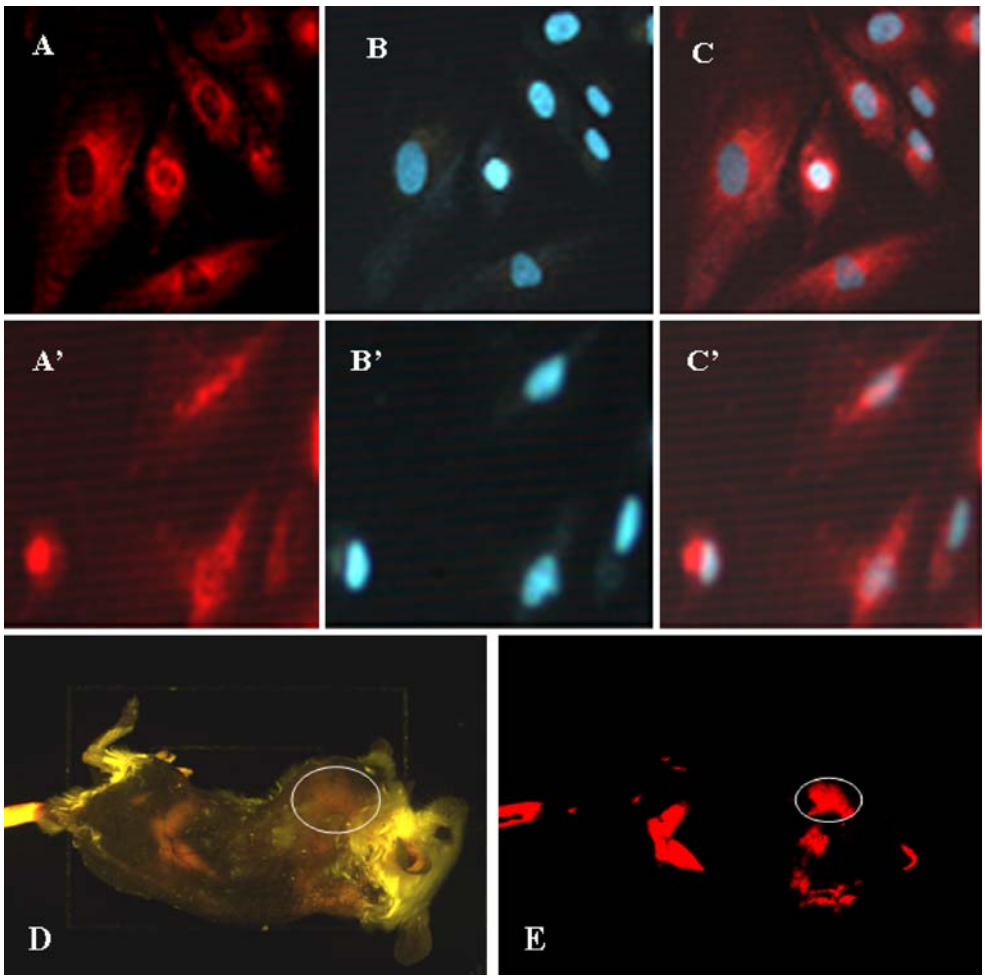

Fig. 5. Distribution of Nile red encapsulated in nanoemulsion *in vitro* and *in vivo*. Upper panel: Fluorescence microscopy images of Nile red and Hoechst 33342 in the same A549 cells. A549 cells were incubated with Nile red dissolved in HBSS containing 1% DMSO for 0.5 h (*A*), and followed by incubation with Hoechst 33342 in HBSS (2 μg/ml) for 10 min (*B*), then *A* and *B* were overlapped (*C*) to detect the distribution of Nile red in A549 cells with cell nucleus stained blue by Hoechst 33342; the same operation using Nile red nanoemulsion in place of Nile red solution (*A′*, *B′*, and *C′*). *Lower panel In vivo* fluorescence image of Nile red in depilated mice bearing S180 cells (tumor location were *circled* in the figures with ellipse curve) at 90 min after intravenous administration of Nile red nanoemulsion (*D*). *E* represents schematic diagram of *D* after some dispositions.

from tumors in mice could be observed under MATSTRO live animal multispectral imaging system (CRI Co.) after i.v. administration of Nile red nanoemulsion.

DISCUSSION

Drug solubility in lipid vehicle is affected by many factors such as microstructure, droplet size, interfacial nature and physicochemical properties of the oil, surfactant, and the drug, etc (24). Meanwhile, it is generally helpful to determine solubility of drug in water and various oils before preparing emulsions. Although MONCPT is nearly insoluble as mentioned above, a prominent increased solubility of MONCPT in small molecular short-chain triglycerides was observed to be 42.25 μg/ml in tributyrin and even 155.62 μg/ml in triacetin. However, the results obtained by us showed that not much MONCPT could be dissolved in the emulsions composed of tributyrin or triacetin as oil phase (data not shown), which may be resulted from the fact that the increase in solubility of drug loaded in emulsion is related not only the nature of oil, but also the location of hydrophobic drug at the interface of the emulsion. It's reported that depending upon the nature of the oil, in particular its size relative to the hydrophobic chain of the surfactant, the oil, especially the smaller oils which act like co-surfactants may penetrate into the surfactant tails of the interfacial monolayer (16,25). This cause a dilution of the polyoxyethylene chain containing region close to the hydrophobic core of the micelle and destroys one of the main loci of drug solubilization, which counterbalances the higher bulk solubility in such oils. In contrast, the oils with larger molecular volume could form a distinct core and do not penetrate through the surfactant interface (16,24). With view to the above, soybean oil was used as the oil phase in the emulsion in this study to avoid the potential adverse effects offered by tributyrin and triacetin. Increased solubility of MONCPT in soybean oil could be achieved when lipoid E-80 was added as surfactant, probably for the interaction between MONCPT and surfactant or other transformation of microstructure. Cremophor EL, another surfactant with potent surface activity, was added and mixed with lipoid E-80 to obtain a stable, homogeneous nanoemulsion with hypoviscosity. As a whole, MONCPT nanoemulsion was prepared by microfluidization using Lipoid E-80 and cremophor EL as main emulsifiers.

It is interesting and important to elucidate the mechanism of solubility enhancement offered by nanoemulsion. Being a solvatochromic probe which is capable of exhibiting a large shift in the wavelength of maximum absorbance (λ_{max}) in various solvents, Nile red was used recently in investigating the solubility and micropolarity of emulsion (22) based on the fact that λ_{max} of Nile red changes significantly upon an increase in the polarity of the microenvironment. For example, the λ_{max} shifts from 593.2 nm in water to 545.6 nm in 1-propanol and down to 521.6 nm in toluene as reported (26). As shown in Fig. 2, much more Nile red may be located at the surfactants interface between oil phase and water phase. Both MONCPT and Nile red are hydrophobic and nearly insoluble in water. But different from Nile red, MONCPT has only a very limited solubility in oils, which is water-insoluble and oil-insoluble with a P value 3.82±1.31. In comparison to Nile red that is located and accumulated in oil phase preferentially and then located in surfactants interface, it is conceivable that most of MONCPT may locate in surfactants interface of the nanoemulsion, which is indirectly confirmed by the fact that the solubility of MONCPT in nanoemulsion is significantly higher than that in water and oil.

One of the desired characteristics of a drug delivery vehicle is to provide sustained release of the incorporated drug to obtain prolonged effects and avoid high concentration in blood (27), especially for those drugs that are quickly eliminated from body such as some camptothecin derivatives, e.g. hydroxycamptothecin, 9-nitro-camptothecin etc (28). The reversed-dialysis bag method was applied for its advantage of favourable imitation *in vivo* when nanoemulsion was injected bolus intravenously and diluted rapidly by blood in body. And a relatively sustained release was observed for MONCPT nanoemulsion as shown in Fig. 1. On the whole, the protection and sustained release of MONCPT could be attributed to the entrapment of MONCPT in the nanoemulsion. Meanwhile, no significant change of pKa value, a dissociation equilibrium constant reflecting the essential characteristic of compound and being calculated from the process of lactones form of MONCPT transformed into carboxylate form in different pH solutions, was observed in nanoemulsion (pKa=6.51) compared to that in water solution (pKa=6.45).

The mechanism of anti-tumor activity of MONCPT is associated with antiangiogenesis response and regulation of cell cycle described previously by us (7,8). Our results here demonstrated that MONCPT encapsulated in nano-carrier did not change the effect on cell cycle induced by drug itself. On the other hand, similar with other camptothecin derivatives, loss of activity of MONCPT was caused by the transformation of molecule structure into the water-soluble salts when the drug dissolved in alkaline solution when injected intravenously (9–11), which accounts for the decreased anti-tumor activity of MONCPT injection in both *in vitro* and *in vivo* experiments. In contrast to solution, nanoemulsion represents a way of sustained drug release way that can stabilize the blood drug level and offer a prolonged effect to an extent, which is favorable to the *in vivo* therapeutic effect of drug. However, it may cause no significant difference between solution and nanoemulsion in the *in vitro* anti-tumor activity because of the continuous contact of cells with drug that dissolved in either solution or nanoemulsion. Meanwhile, it was reported that an enhanced membrane permeability or increased efficacy of drug could be achieved by the utilization of nanoemulsion owing to its decreased particle size, or interference of components in nanoemulsion with cell membrane (29,30). Therefore, it may be employed in the nuclear gene delivery systems to achieve nuclear transport of drug (31), which was further demonstrated by the fact that Nile red incorporated in the nanoemulsion could be transported into cell nucleus as showed in the present study. As both Nile red and MONCPT are hydrophobic and could be extrapolated to be difficult to transport across hydrophilic nuclear membrane into nucleus, this capability of nanoemulsion to deliver Nile red into nucleus to some extent may be also helpful to elucidate the difference of *in vitro* antitumor activity between nanoemulsion and aqueous solution in the present study.

We have studied both *in vitro* and *in vivo* anti-tumor activity of MONCPT on A549 cells as reported (8), and then

focus our present study (such as anti-tumor activity) on the S180 tumor.

Mechanism of enhanced *in vivo* anti-tumor activity for nano-carrier involves not only the enhanced membrane permeability, distribution of hydrophobic molecule into the cell nucleus, prolonged effects and decreased side effects owing to the enhanced solubility and sustained release of drug, but also some other potential factors, such as increased accumulation or target of drug in tumor tissues *via* the EPR effect based on the distribution of particle size of nano-carrier (32,33). *In vivo* imaging indicated that the nanoemulsion prepared in the current work might enhance the delivery of drug into tumor. Taken together, the nanoemulsion provides a promising carrier for MONCPT in future anti-tumor research though there still many mechanisms remain to be elucidated.

ACKNOWLEDGEMENTS

The study was supported in part by Scientific Research Fund of Ministry of Health-Medical Science Critical Technological Program of Zhejiang Province, by the Health Bureau of Zhejiang Province Foundation (No. WKJ2008-2-029), Zhejiang Provincial Program for the Cultivation of High-level Innovative Health Talents, and Zhejiang Provincial Natural Science Foundation of China (Y207259).

REFERENCES

1. C. H. Takimoto, J. Wright, and S. G. Arbuck. Clinical applications of the camptothecins. *Biochim. Biophys. Acta*. **1400**:107–119 (1998).
2. O. Lavergne, and D. C. Bigg. The other camptothecins: recent advances with camptothecin analogues other than irinotecan and topotecan. *Bull. Cancer.* **12**:51–58 (1998).
3. U. Vanhoefer, W. Achterrath, S. Cao, S. Seeber, and Y. M. Rustum. Irinotecan in the treatment of colorectal cancer: clinical overview. *J. Clin. Oncol.* **19**:1501–1518 (2001).
4. Z. S. Cao, K. Armstrong, M. Shaw, E. Petry, and N. Harris. Nitration of camptothecin with various inorganic nitrate salts in concentrated sulfuric acid: a new preparation of anticancer drug 9-nitrocamptothecin. *Synthesis*. **12**:1724–1730 (1998). doi:10.1055/s-1998-2207.
5. M. C. Wani, A. W. Nicholas, and M. E. Wall. Plant antitumor agents .23. Synthesis and antileukemic activity of camptothecin analogues. *J. Med. Chem.* **29**:2858–2863 (1986). doi:10.1021/jm00161a035.
6. M. Gao, K. D. Miller, G. W. Sledgeb, and Q. H. Zheng. Radiosynthesis of carbon-11-labeled camptothecin derivatives as potential positron emission tomography tracers for imaging of topoisomerase I in cancers. *Bioorg. Med. Chem. Lett.* **15**:3865–3869 (2005). doi:10.1016/j.bmcl.2005.05.108.
7. X. C. Yang, P. H. Luo, B. Yang, and Q. J. He. Antiangiogenesis response of endothelial cells to the antitumour drug 10-methoxy-9-nitrocamptothecin. *Pharmacol. Res.* **54**:334–340 (2006). doi:10.1016/j.phrs.2006.06.001.
8. P. H. Luo, Q. J. He, X. G. He, Y. Z. Hu, W. Lu, Y. Y. Cheng, and B. Yang. Potent antitumor activity of 10-methoxy-9-nitrocamptothecin. *Mol. Cancer. Ther.* **54**:962–968 (2006). doi:10.1158/1535-7163.MCT-05-0385.
9. C. J. Thomas, N. J. Rahier, and S. M. Hecht. Camptothecin: current perspectives. *Bioorg. Med. Chem.* **12**:1585–1604 (2004). doi:10.1016/j.bmc.2003.11.036.
10. J. J. Zhou, J. Liu, and B. Xu. Relationship between lactone ring forms of HCPT and their antitumor activities. *Acta. Pharmacol. Sin.* **22**:827–830 (2001).
11. R. P. Hertzberg, M. J. Caranfa, K. G. Holden, D. R. Jakas, G. Gallagher, M. R. Mattern, S. M. Mong, J. O. Bartus, R. K. Johnson, and W. D. Kingsbury. Modification of the hydroxy lactone ring of camptothecin: inhibition of mammalian topoisomerase I and biological activity. *J. Med. Chem.* **32**:715–720 (1989). doi:10.1021/jm00123a038.
12. S. Kawakami, F. Yamashita, and M. Hasida. Disposition characteristics of emulsions and incorporated drugs after systemic or local injection. *Adv. Drug Deliv. Rev.* **45**:77–88 (2000). doi:10.1016/S0169-409X(00)00102-2.
13. P. P. Constantinides, K. J. Lambert, A. K. Tustian, B. Schneider, S. Lalji, W. Ma, B. Wentzel, D. Kessler, D. Worah, and S. C. Quay. Formulation development and antitumor activity of filter-sterilizable emulsion of paclitaxel. *Pharm. Res.* **17**:175–182 (2000). doi:10.1023/A:1007565230130.
14. J. Rossi, S. Giasson, M. N. Khalid, P. Delmas, C. Allen, and J. C. Leroux. Long-circulation poly (ethylene glycol)-coated emulsions to target solid tumors. *Eur. J. Pharm. Biopharm.* **67**:329–338 (2007). doi:10.1016/j.ejpb.2007.03.016.
15. K. Zurowska-Pryczkowska, M. Sznitowska, and S. Janicki. Studies on the effect of pilocarplne incorporation into a submicron emulsion on the stability of the drug and the vehicle. *Eur. J. Pharm. Biopharm.* **47**:255–260 (1999). doi:10.1016/S0939-6411(98)00098-8.
16. M. J. Lawrence, and G. D. Rees. Microemulsion-based media as novel drug delivery systems. *Adv. Drug Deliv. Rev.* **45**:89–121 (2000). doi:10.1016/S0169-409X(00)00103-4.
17. O. Sonneville-Aubrun, J. T. Simonnet, and F. l'Alloret. Nanoemulsions: a new vehicle for skincare products. *Adv. Colloid Interface Sci.* **108–109**:145–149 (2004). doi:10.1016/j.cis.2003.10.026.
18. L. A. Pires, R. Hegg, C. J. Valduga, S. R. Graziani, D. G. Rodrigues, and R. C. Maranhao. Use of cholesterol-rich nanoparticles that bind to lipoprotein receptors as a vehicle to paclitaxel in the treatment of breast cancer: pharmacokinetics, tumor uptake and a pilot clinical study. *Cancer Chemother Pharmacol.*, in press (2008) http://www.springerlink.com/content/t1452120506h7327/.
19. D. Attivi. Formulation of insulin-loaded polymeric nanoparticles using response surface methodology. *Drug DeV. Ind. Pharm.* **31**:179–189 (2005). doi:10.1081/DDC-200047802.
20. L. Copolovici, and U. Niinemets. Salting-in and salting-out effects of ionic and neutral osmotica on limonene and linalool Henry's law constants and octanol/water partition coefficients. *Chemosphere*. **69**:621–629 (2007). doi:10.1016/j.chemosphere.2007.02.066.
21. M. Y. Levy, and S. Benita. Drug release from submicronized o/w emulsion: new *in vitro* kinetic evaluation model. *Int. J. Pharm.* **66**:29–37 (1990). doi:10.1016/0378-5173(90)90381-D.
22. M. B. Moshe, S. Magdassi, Y. Cohen, and L. Avram. Structure of microemulsions with Gemini surfactant studied by solvatochromic probe and diffusion NMR. *J. Colloid Interface Sci.* **276**:221–226 (2004). doi:10.1016/j.jcis.2004.03.015.
23. P. Skehan, D. Scudiero, R. Storeng, A. Monks, J. McMahon, D. Vistica, J. T. Warren, H. Bokesch, S. Kenney, and M. R. Boyd. New colorimetric cytotoxicity assay for anticancer-drug screening. *J. Nat. Cancer Inst.* **82**:1107–1112 (1990). doi:10.1093/jnci/82.13.1107.
24. S. S. Rane, and B. D. Anderson. What determines drug solubility in lipid vehicles: is it predictable. *Adv. Drug Del. Rev.* **60**:638–656 (2008). doi:10.1016/j.addr.2007.10.015.
25. C. Malcolmson, C. Satra, S. Kantaria, A. Sidhu, and M. J. Lawrence. Effect of oil on the level of solubilization of testosterone propionate into nonionic oil-in-water microemulsions. *J. Pharm. Sci.* **87**:109–116 (1998). doi:10.1021/js9700863.
26. H. Kunieda, N. Masuda, and K. Tsubone. Comparison between phase behavior of anionic dimeric (Gemini-Type) and monomeric surfactants in water and water-oil. *Langmuir.* **16**:6438–6444 (2000). doi:10.1021/la0001068.
27. F. Liu, and D. Liu. Long-circulating emulsions (oil-in-water) as carriers for lipophilic drugs. *Pharm. Res.* **12**:1060–1064 (1995). doi:10.1023/A:1016274801930.
28. D. F. Zhong, K. Li, J. H. Xu, Y. Du, and Y. F. Zhang. Pharmacokinetics of 9-nitro-20(S)-camptothecin in rats. *Acta Pharmacol. Sin.* **24**:256–262 (2003).

29. P. K. Ghosh, and R. S. R. Murthy. Microemulsions: a potential drug delivery system. *Curr. Drug Deliv.* **3**:167–180 (2006). doi:10.2174/156720106776359168.
30. J. B. Tagne, S. Kakumanu, D. Ortiz, T. Shea, and R. J. Nicolosi. A nanoemulsion formulation of tamoxifen increases its efficacy in a breast cancer cell line. *Mol. Pharm.* **5**:280–286 (2008). doi:10.1021/mp700091j.
31. T. Masuda, H. Akita, T. Nishio, K. Niikura, K. Kogure, K. Ijiro, and H. Harashima. Development of lipid particles targeted *via* sugar-lipid conjugates as novel nuclear gene delivery system. *Biomaterials*. **29**:709–723 (2008). doi:10.1016/j.biomaterials.2007.09.039.
32. W. Junping, K. Takayama, T. Nagai, and Y. Maitani. Pharmacokinetics and antitumor effects of vincristine carried by microemulsions composed of PEG-lipid, oleic acid, vitamin E and cholesterol. *Int. J. Pharm.* **251**:13–21 (2003). doi:10.1016/S0378-5173(02)00580-X.
33. B. A. Teicher. Molecular targets and cancer therapeutics: discovery, development and clinical validation. *Drug Resist Updat.* **3**:67–73 (2000). doi:10.1054/drup.2000.0123.